

# Implementation of an energy management strategy with drivability constraints for a dual motor electric vehicle

**Abstract:** This paper presents a real-time energy management strategy to distribute the power demand between two independent motors properly. Based on the characteristics of the novel transmission system, an enumeration based searching approach is used to hunt for the optimal working points for both motors to maximize the overall efficiency. Like many energy management strategies, approaches that focus on reducing energy consumption can result in frequent gearshifts. To improve drivability and make a balance between energy consumption and gearshifts, a cost function is designed. To verify the effectiveness of the proposed method, a mathematical model is built and the simulation results demonstrate the achieved improvements.

**Keywords:** electric vehicles; dual motor system; energy management strategy; frequent gearshifts

---

## 1. Introduction

As the energy resource shortage is becoming increasingly serious, vehicle industry is facing an unprecedented challenge [1-3]. Due to the rising price of traditional energy like fossil fuel and the penalty agreement on green gas emissions globally, the traditional transportation industry is transferring to electrical ways which are more efficient in the energy usage and more environmentally friendly. As a consequence, researchers and manufacturers pay more attention to hybrid electric vehicles and pure electric vehicles which brings more sustainable economy, cleaner usage of energy and better driving comfort [4]. However, the low energy-storage capacity of the batteries limits the driving distance significantly leading to the unsuccessful popularization of EVs in the commercial market[5]. Therefore, measures should be taken in every possible way to make the most of the energy [6, 7].

Transmission is fundamental to realize a high-efficiency electric powertrain with little compromise of driving ability[8, 9]. Up to now, the research has tended to focus on the application of multi-speed transmission rather than single-speed transmission. Extensive research has shown that the motor size can be reduced by applying multi-speed transmissions to electric vehicle platforms, as well as achieving the desired power by providing a wider speed range of usable torque and reducing energy consumption by gear-shifting[10]. In all current kinds of multi-speed transmission, AMT stands out as a proper choice of electric vehicle transmissions due to the advantages of the mature technique, reliable running performance and good efficiency[11]. Besides, it also has a low manufacture cost and compact size[12]. The disadvantages of this transmission system cannot be ignored like vibration and torque interruption while shifting, as well as the losses of clutch result from significant wear[13, 14].

However, these drawbacks can be improved in electric vehicles, because electric motors have a controllable actuating speed which makes it possible to run a clutch-less transmission system in electric vehicles to minimize the additional losses[11, 15, 16]. Moreover, to eliminate the torque interruption of AMT, a dual motor platform is used to fill the torque hole during shifting with another motor[17-19].

The power distribution is important in energy management besides the structure of the powertrain[20]. Related researches are developing fast in diverse ways. The rule-based control strategy is the most common and simplest control method. Its advantages are the high computing speed, simple architecture and well control performance like [21, 22]. The fuzzy logic control strategy is good at balancing the efficiency of whole powertrain components since this method can allow the

possibility of imprecise measurements and uncertain changes between components [23, 24]. Global optimization-based control strategy such as stochastic dynamic programming (SDP) uses an improved computing method, making the best decisions according to the results which come from the former problems into the next situation till the end, such as [25, 26]. Model predictive control (MPC) incorporates the future driving load in the predictive model to manage the upcoming driving status[27]. The main weakness of these theories is that the optimal solution depends highly on pre-known knowledge so that it is difficult for the application of real driving conditions that are full of uncertainty. Equivalent consumption minimization strategy (ECMS) transfers the electric energy consumption to fuel consumption by using an equivalent factor[28]. However, it cannot be used in the dual-motor input structure since the battery supporting both motors is working as the only power source without power transfer problems. As a result, a specific energy management strategy is designed using enumeration algorithm.

It is worth noting that most studies in the energy management field have only focus on the optimization of energy consumption while failing to address the drivability attributes. Excessive gear shifting [29] is one of the most typical problems encountered by energy management strategies as achieving the best efficiency inherently requires frequent gear changes. To solve this problem, a specific shifting stability control approach is proposed. It employs a bump function to both controls the minimum shifting frequency and reveals the relationship between the shifting frequency and the shifting cost penalty. As there are two parameters which are the bump amplitude and bump duration in determining the cost function, an advanced optimization strategy which can solve the two-objective problem is adopted [30]. The proposed PSO multi-objective optimization method could generate a pair of desirable parameters according to specific driving condition achieving both low gear shift numbers and low energy consumption.

This paper proposes a real-time energy management strategy to improve the overall efficiency of a dual motor transmission system. Since energy-oriented strategies often lead to frequent gearshifts, an optimization method based on PSO is adopted to filter undesirable gearshifts. The rest paper is organized as the following. In section 2, the powertrain mathematic modeling, and parameter selection of electric motors are introduced. Section 3 presents the designed energy management strategy and cost function for shift stability. Section 4 shows the simulation results of driving cycles. Conclusions are drawn in section 5.

## 2. Powertrain Modelling

To maximize energy efficiency while meeting drivability requirements, a clutchless two motor transmission is utilized. The structure of the transmission system is shown in Fig. 1.

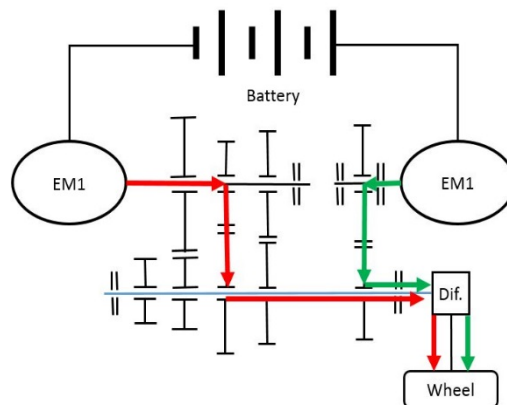


Figure 1. Dual motor transmission.

In the dual input clutchless transmission system, the first motor is connected to a multi-speed transmission. Since electric motors are speed controllable, gearshifts can be achieved without clutches. The combination of motor speed control and synchronizer actuation make it a cost-effective and

efficient way to achieve the merits of multispeed transmission. In order to realize power-on shifting, the second motor helps compensate the torque hole during gearshifts. As the second motor drives the wheels using a fixed reduction ratio, the first and second motors can supplement each other to provide power in some driving conditions.

The battery model based on the DC circuit is used for both motors in this study. This allows for direct model control through the input voltage, and the complexity inherent in power electronics is lost. The differential equation is calculated as:

$$L\dot{I} = K_e\dot{\theta} - RI + V \quad (1)$$

where  $L$  denotes the inductance,  $I$  denotes the line current,  $K_e$  is the electromagnetic field constant,  $R$  is the line resistance, and  $V$  is voltage. The motor torque is calculated as:

$$T = K_T I \quad (2)$$

where  $K_T$  is the torque coefficient. The chief question that must be considered about the motors first is which of the two motors is the primary drive motor and how much power is required. Obviously, the use of multiple speed ratios is beneficial to improving the driving efficiency of the vehicle under a wider speed range, thus it should be considered the primary driving motor. The motor driving the fixed ratio, hereafter EM2, is required to provide additional driving power during certain periods of operation and provide high torque outputs for shifting. If a gear shift is undertaken whilst EM1 is driving the wheels at its peak output torque in any given speed, then the EM2 torque requirements can be defined and the peak power requirements of the motor established. The peak torque for EM2 that should be delivered during a generic up or down shift is defined, excluding any losses in the transmission, as:

$$T_2 = \frac{i_1 i_2}{i_3} T_1 \quad (3)$$

where  $i_1$  is the gear ratio for multispeed transmission,  $i_2$  is the counter shaft gear ration and  $i_3$  is the fixed reduction gear ratio for motor 2. The speed range required for this torque delivery is defined as:

$$N_2 = \frac{i_3}{i_1 i_2} N_1 \quad (4)$$

Obviously, these two equations demonstrate that the speed and torque requirements for any particular gear shift produce identical peak power requirements to the primary driving motor. This is necessarily considered as over design of the motor as this power would only be required for the one to two seconds required for the gear shift. A balance must, therefore, be achieved through a review of the shifting patterns of the vehicle under a typical driving cycle. The motor efficiency maps are shown in Fig. 2.

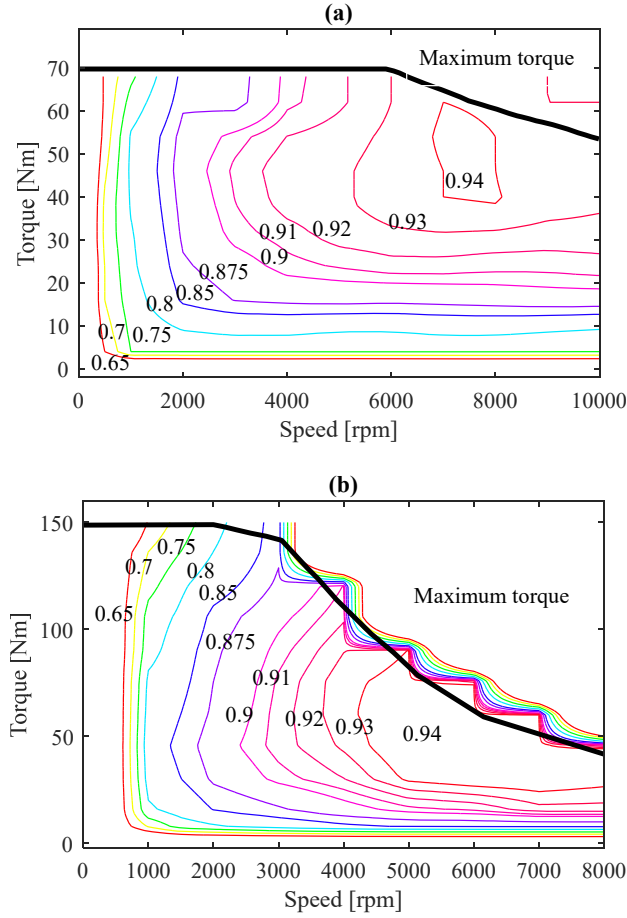


Figure 2. Motor efficiency maps.

The selected gear ratios are shown in Table 1.

Table 1. Gear ratios.

Symbol	Variable name	Value
$i_{c1}$	Counter gear for motor 1	4.62
$i_{c2}$	Counter gear for motor 2	2.16
$i_{g1}$	Gear 1 for motor 1	3.46
$i_{g2}$	Gear 2 for motor 1	2.08
$i_{g3}$	Gear 3 for motor 1	1.32
$i_2$	Reduction gear for motor 2	3.46

These gear ratios are designed to cover most driving conditions. The first and second gear ratio of AMT is set to be relatively high to meet the requirements of urban driving conditions, where the vehicle speed is low and frequent stops are easy to see. By doing this, EM1 can work in a more efficient area by adjusting torque and speed through a large gear ratio. Then, the third gear ratio of AMT, as well as the fixed gear ratio of EM2, is designed to meet the requirements of mid-high speed driving conditions, especially for traveling and highway cruising.

### 3. Energy Management Strategy

In order to maximize energy efficiency while meeting dynamic requirements, the energy management strategy plays an important role to distribute the power flow between two motors. Two motors should work in a supplementary way to achieve a desirable efficiency.

The output power is calculated as the following

$$P_{out} = T_1 * \frac{\dot{\theta}_1}{\eta_1} + T_2 * \frac{\dot{\theta}_2}{\eta_2} \quad (T_1 * \dot{\theta}_1 > 0 \& T_2 * \dot{\theta}_2 > 0) \quad (5)$$

where  $\eta_1$  is efficiencies for first motor and  $\eta_2$  is that for sethe cond motor.

To make the most of the energy, both motors can work as a generator to charge the battery. And the working conditions of regenerative braking is also included as well. Accordingly, the reusable power consumption is calculated as the following

$$P_{in} = T_1 * \frac{\dot{\theta}_1}{\eta_1} + T_2 * \frac{\dot{\theta}_2}{\eta_2} \quad (T_1 * \dot{\theta}_1 < 0 \& T_2 * \dot{\theta}_2 < 0) \quad (6)$$

The overall power consumption is calculated below

$$P = P_{output} + P_{input} \quad (7)$$

In this equation, the variables are the  $T_1$ ,  $T_2$ ,  $\theta_1$ , and  $\theta_2$ . However, they are not independent with each other.

As for the motor torques, the relation between two motors' can be described as

$$T_2 = \frac{J_{eq3} * \bar{\alpha}_{Final} + T_v - i_1 * (T_1 - J_{eq1} * \bar{\alpha}_1)}{i_2} + J_{eq2} * \bar{\alpha}_2 \quad (8)$$

where  $J_{eq1}$  is the equivalent inertia for first motor driveline,  $J_{eq2}$  is for second motor driveline and  $J_{eq3}$  is for the vehicle body. The  $\bar{\alpha}_{Final}$ ,  $\bar{\alpha}_1$ ,  $\bar{\alpha}_2$  are the demanded angular acceleration for the first motor, second motor and final shaft individually. Once one of the motor torque is decided, the other motor torque can be settled down. In this study,  $T_1$  is used as the independent variable.

As to the speed, once the driving speed is given, the speeds of two motors are decided by the corresponding gear ratio. The equation can be expressed as below

$$\dot{\theta}_{EM1} = \frac{\bar{v}}{R_w} \cdot i_1, \dot{\theta}_{EM2} = \frac{\bar{v}}{R_w} \cdot i_2 \quad (9)$$

Therefore, the independent variable in this system is the torque of EM 1 and the corresponding gear ratio. As a result, the objective function is as below

$$\min P(T_1, i) \quad (10)$$

subject to

$$\begin{cases} -\dot{\theta}_{1,max} \leq -\dot{\theta}_1 \leq \dot{\theta}_{1,max} \\ -T_{1,max}(\dot{\theta}_1) \leq T_1 \leq T_{1,max}(\dot{\theta}_1) \\ -\dot{\theta}_{2,max} \leq -\dot{\theta}_2 \leq \dot{\theta}_{2,max} \\ -T_{2,max}(\dot{\theta}_2) \leq T_2 \leq T_{2,max}(\dot{\theta}_2) \end{cases}$$

Since the battery is the only power source, there are no energy transfer issues. The enumerating method can reduce the computational burden while being as close as possible to the optimal solutions. In the design space, the independent variable  $T_{M1}$  is discretized into a regular dense grid points of 2 Nm intervals. At these discretized points, the objective function value  $P$  are calculated under constraints. The optimal points with minimum objective values will be chosen as the final results after excluding the unfeasible points. Fig. 3 shows the plots of the objective function, it can be seen that the trajectory of the optimal solutions would be adjusted under different driving conditions.

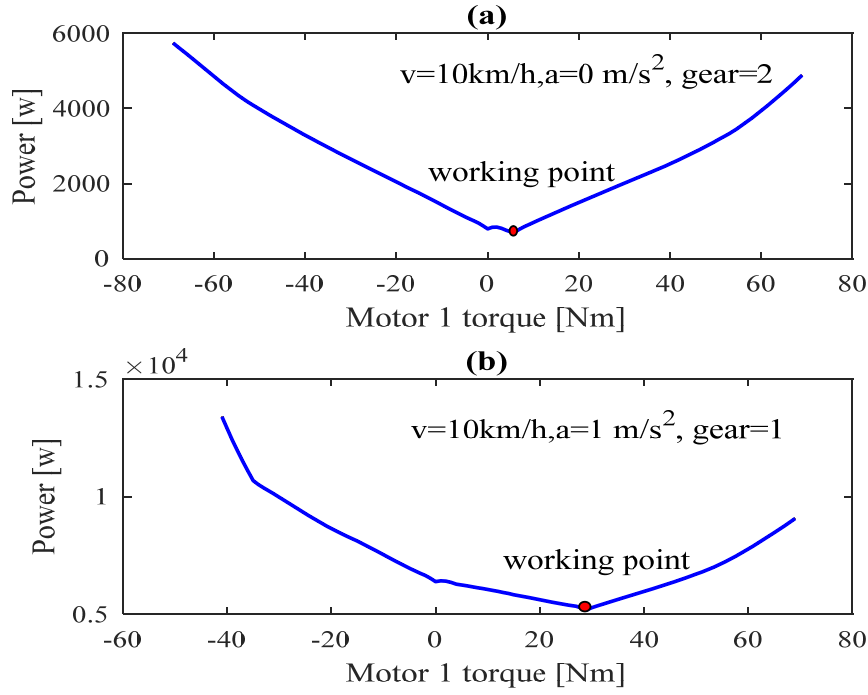


Figure 3. Objective function value of different driving conditions.

#### 4. Shifting Stability

The energy management strategy can provide optimal power distribution between two motors, but it can also lead to frequent gear-shifting. To avoid this problem, a cost function is used in the proposed energy management strategy to improve shift stability. It is defined as the following

$$f_{cost} = A * e^{-\frac{1}{1-x^2}} \quad (11)$$

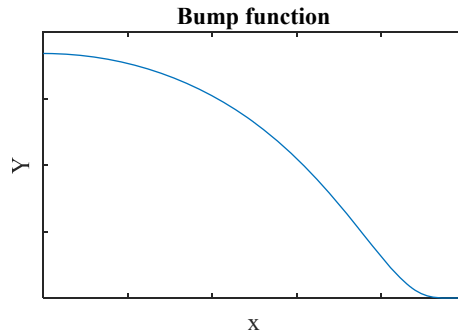
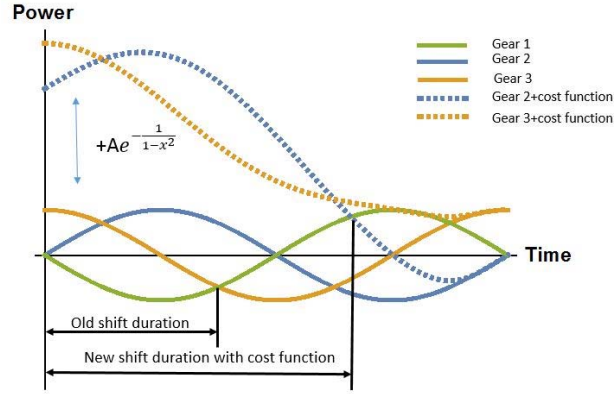


Figure 4. Feature of Bump function.

The bump function is introduced as a penalty to solve the problem of frequent gearshifts. As shown in Fig. 4, the penalty will start from a large value in the early period, then decreasing smoothly but fast to zero.

Fig. 5 shows the schematic diagram of the designed cost function where the solid lines denote the power consumption for each gear. Since the power consumptions of different gear states are not the same, the optimal gear is decided by searching for the gear ratio with minimum power consumption. Based on this, the gear will change with the lowest curves to save energy, which results in a short shifting duration. With the designed cost function, every time gear-shifting completes, the power consumption of the current gear will keep its value, but the rest gears will be imposed additional penalty values. From Fig.5, the working gear changes from the blue line to the gear line in the beginning, so that the nonworking gear will be imposed a penalty due to the cost function. Thus,

the shifting duration last for a longer period when searching for minimum power consumption and frequent gearshifts are significantly reduced.



**Figure 5.** The schematic diagram of the designed cost function.

Considering the shifting stability, the objective function to be minimized in the energy management strategy will be defined as

$$P_{sub\_opt} = P + f_{cost} \quad (12)$$

However, since the gear-shifting directed by energy management strategy aims at achieving high energy efficiency, the reduction of gear changes will lead to an increase in power consumption. To filter out unnecessary shifts while minimizing the extra energy consumption, the coefficients of the cost function is the key. In order to make a balance between energy consumption and gearshifts, the optimization approach based on Particle Swarm Optimization is used to optimize the corresponding coefficients.

PSO algorithm is a heuristic optimization algorithm that simulates the random distribution and instinct behavior of creatures, which are called particles. Particles interact with each other and move as a group, affecting the overall speed and location of all groups. The key element of PSO is the speed and position of swarms, which is defined as follows:

$$V_{id}^{k+1} = \omega V_{id}^k + c_1 r_1 (P_{id}^k - X_{id}^k) + c_2 r_2 (P_{id}^k - X_{id}^k) \quad (13)$$

$$X_{id}^{k+1} = X_{id}^k + V_{id}^{k+1} \quad (14)$$

where  $\omega$  is the inertial weight,  $k$  is the current number of iteration,  $V_{id}$  is the swarm speed,  $X_i$  is the fitness value,  $c_1$  and  $c_2$  are the non-negative constant, called the acceleration factor,  $r_1$  and  $r_2$  are random numbers between 0 and 1. The control configuration is shown in Fig. 6.

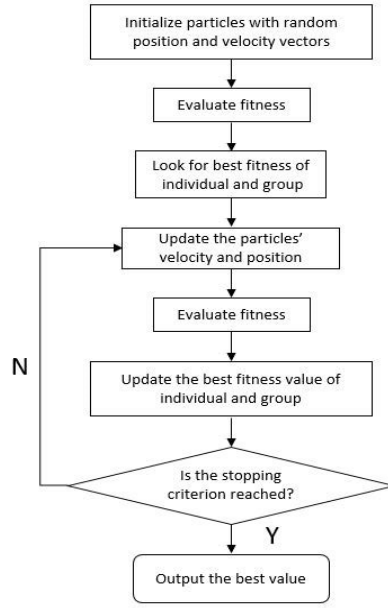


**Figure 6.** Multi-objective optimization control configuration.

In the PSO multi-objective optimization, the functions to be minimized are as below

$$f_1 = \min P(T_1, i) + A * e^{-\frac{1}{1-x^2}} \quad (15)$$

$$f_2 = \min \sum \text{Gearshifts} \quad (16)$$

Because the  $f_1$  and  $f_2$  are not on the same order of magnitude, the values are normalized as below

$$f'_{1k} = \frac{f_{1k}}{\bar{f}_1} \quad (17)$$

$$f'_{2k} = \frac{f_{2k}}{\bar{f}_2} \quad (18)$$

Where  $f_{1k}$  denotes the value for kth generation,  $\bar{f}_1$  denotes the average value.

It worth noting that the PSO optimization is used to determine the coefficients of the cost function off-line. The optimization results will be used in the on-line power-sharing strategy to help calculate the penalty instantaneously.

## 5. Performance Evaluation

### 5.1 Power-sharing strategy evaluation

In order to demonstrate the effectiveness of the proposed power-sharing strategy, the LA92 driving cycle is adopted. The total distance of LA-92 is 15.8km in 1435s. It is a representation of urban driving patterns for light-duty vehicles.

As a comparison, different fixed power distribution strategies are conducted. Fig. 7 shows the energy consumption comparisons.



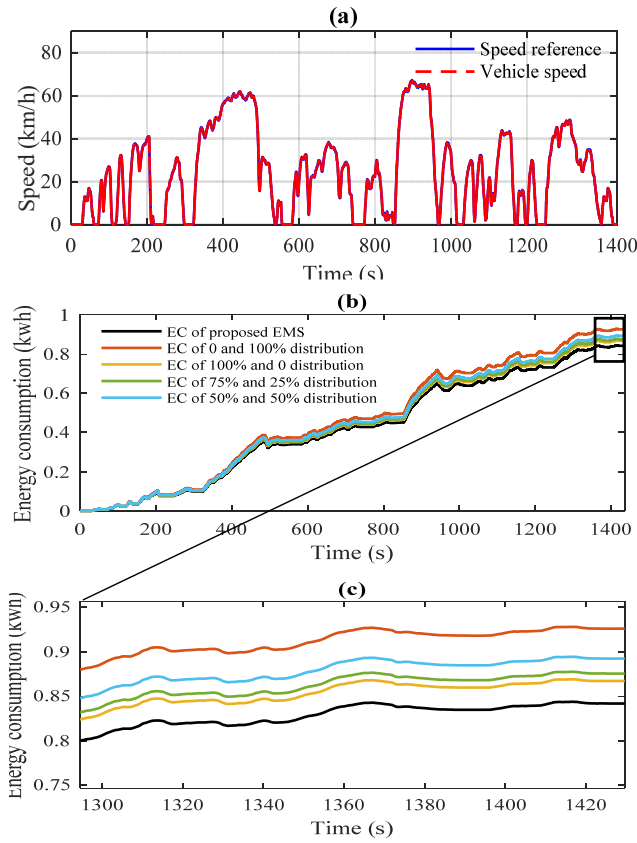


**Figure 7.** Energy consumption comparisons.

Fig. 7(a) shows that there are many starts and stops along the LA-92 driving cycle, which is shown in the form of speed peaks. From the speed file, the proposed energy management strategy can direct the vehicle to follow the target speed accurately. In Fig. 7 (b), fixed distribution strategies are used to make a comparison. The trajectory of energy consumptions is not monotonically increasing because the motors can work as a generator in braking. The results show that the designed energy management strategy achieves the highest efficiency, where two motors are easy to work in their high-efficiency region with proper power distribution. Two motors can work in a supplementary way to provide power. The fixed distributions limit the possibility of optimal solutions. Two motors can hardly achieve their high-efficiency region simultaneously due to distribution constraints. The detailed energy consumption are shown in Table 2.

**Table 2.** Energy consumption comparison.

LA-92	Energy consumption	Extra EC
Proposed strategy	0.8418 kwh	
Motor 1(100%) Motor 2(0%)	0.8726 kwh	3.66 %
Motor 1(75%) Motor 2(25%)	0.8761 kwh	4.07 %
Motor 1(50%) Motor 2(50%)	0.8847 kwh	5.10 %
Motor 1(0%) Motor 2(100%)	0.9252 kwh	9.91 %

It is worth noting that when the higher distribution weight the first motor has, the higher efficiency it brings. As shown in Table 2, the fixed distribution strategies follow up by only motor 1 works (motor 1(100%) motor 2(0%)), 75% of motor 1 and 25% of motor 2, then 50% of motor 1 and 50% of motor 2, then only motor 2 works. This is because of the advantage of multispeed transmission. Since motor 1 is connected to a multi-speed transmission, the energy efficiency can be improved through gear changes, especially in complex and changeable driving conditions. On the other hand, when it comes to stable driving conditions like cruising, the energy efficiency will increase with the weight of the second motor. This is because the second motor works better in low torque high speed

regions. So for different driving situation, the designed power-sharing strategy can always find a decent power distribution ratio to achieve a higher energy efficiency.

## 5.2 Drivability evaluation

Fig. 8 shows the corresponding shifting performance and motor speeds.

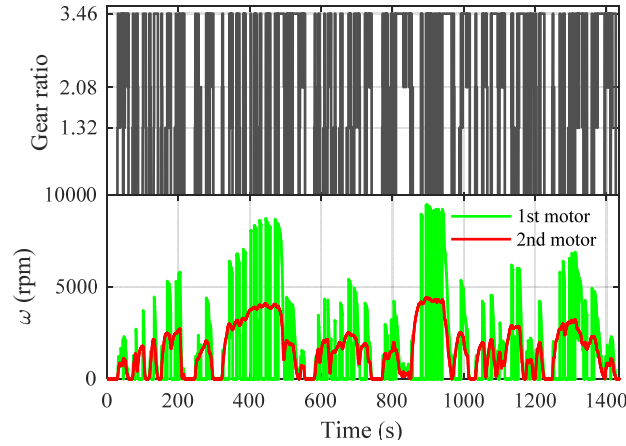


**Figure 8.** Gear shifting with the power-sharing strategy.

It can be seen that, in order to achieve high overall efficiency, the gear kept changing throughout the whole process which introduces parasitic energy losses and uncomfortable driving experiences. Besides, the motor speed figure shows that both motor help to provide power with the proposed strategy. When the vehicle speed is lower than 40km/h, the first motor work as the main power source. The motor speed is high to achieve high efficiency according to the motor efficiency map. Besides, the multispeed transmission can provide high launching torque without compromising efficiency at high operating speed. When the vehicle speed is beyond 40km/h, the second motor will help to provide power with low torque and high speed to guarantee the optimal efficiency.

The motor speed figure demonstrates that motor 1 mainly works when the vehicle speed is below while the motor speed is high to achieve high efficiency. In low speed conditions, the motor 1 works together with AMT to achieve high economic efficiency, because AMT provides high starting torque without compromising the efficiency at high operating speed. When the vehicle speed is above 40km/h, motor 2 will take over to provide power due to the design of the fixed gear ratio for motor 2.

To alleviate the frequent gearshifts, the optimized cost function is adopted and the improved shifting performance is shown in Fig.9.

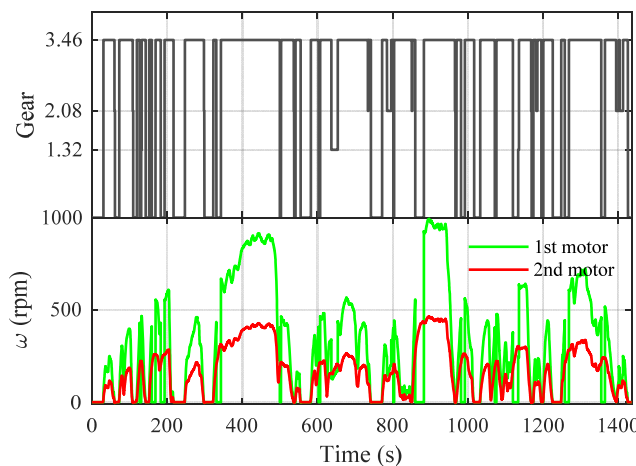


**Figure 9.** Gear shifting with the modified power-sharing strategy.

Compared to Fig. 8, the shifting frequency has been greatly reduced. The motor speed file shows that the performance of the first motor works in a steady and continuous way with less frequent launching and stopping.

**Table 3.** Drivability improvement and energy consumption.

LA-92	Before	After
Gear shifts	392	75
Average shifting duration	4s	19s
Shifts last less than 2s	254	22
Energy consumption	0.8418 kwh	0.8519 kwh

Table 3 explicates the drivability improvement and compares the sub-optimality of energy consumption. The energy-oriented power-sharing strategy causes 392 shifts in the LA-92 driving cycle with one shift every 4 seconds on average. Moreover, many gear states lasts for less than 2 seconds. In comparison, with the help of shifting stability control the shifts reduce to 75 with one shift every 19s on average. The shift duration is expanded almost 5 times larger and the shifts last too short time is significantly reduced. However, the reduction of gear shifts gives rise to the sub-optimal energy consumption, which rising from 0.8418 kWh to 0.8519 kWh.

Fig. 10 shows the power consumption under shift stability control. It can be seen that the significant reduction of gearshifts only leads to 1.2% extra power consumption.

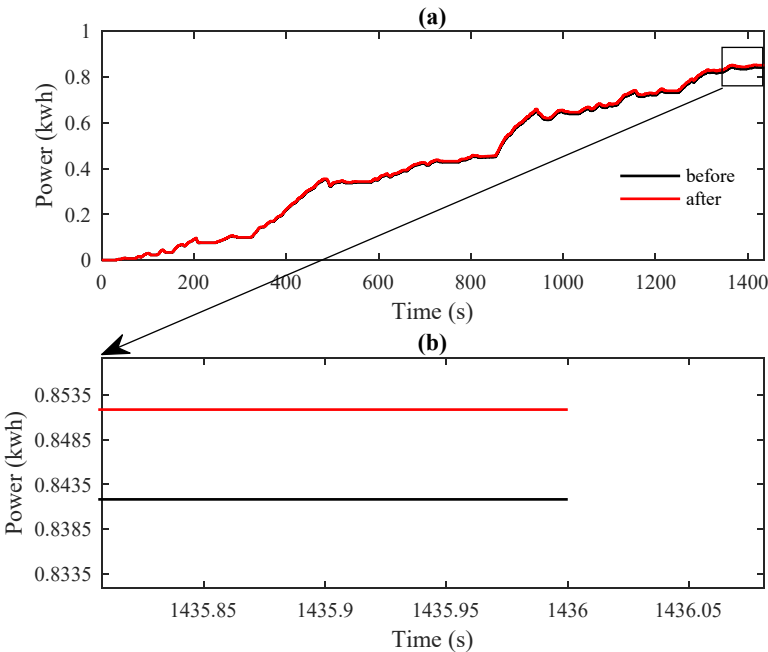


**Figure 10.** Power consumption with and without shift stability control.

### 5. Conclusion

This paper presents a real-time power-sharing strategy with the corresponding shifting stability control algorithm for a new dual input clutchless transmission system. The power-sharing strategy could adequately distribute the power demand to the motors in the system achieving a relatively high overall efficiency. To solve the inherent frequent shifting problem, a decent cost function is designed which considers both the minimum gear change duration and the interval between two adjacent gear shifts. To optimize the overall efficiency and the gear shift frequency, and multi-objective optimization method is proposed which decides both the amplitude and the duration of the cost function. A detailed mathematic model has been built and the improvements achieved by the proposed system are verified.

## 306    **References**

- 307    [1]    E. Apostolaki-Iosifidou, P. Codani, and W. Kempton, "Measurement of power loss during  
308        electric vehicle charging and discharging," *Energy*, vol. 127, pp. 730-742, 2017.
- 309    [2]    Z. Junzhi, L. Yutong, L. Chen, and Y. Ye, "New regenerative braking control strategy for  
310        rear-driven electrified minivans," *Energy Conversion and Management*, vol. 82, pp. 135-145,  
311        2014.
- 312    [3]    P. Fajri, S. Lee, V. A. K. Prabhala, and M. Ferdowsi, "Modeling and integration of electric  
313        vehicle regenerative and friction braking for motor/dynamometer Test Bench Emulation,"  
314        *IEEE Transactions on Vehicular Technology*, vol. 65, pp. 4264-4273, 2016.
- 315    [4]    M. Cipek, D. Pavković, and J. Petrić, "A control-oriented simulation model of a power-split  
316        hybrid electric vehicle," *Applied energy*, vol. 101, pp. 121-133, 2013.
- 317    [5]    B. Nykvist and M. Nilsson, "Rapidly falling costs of battery packs for electric vehicles,"  
318        *Nature climate change*, vol. 5, p. 329, 2015.
- 319    [6]    M. Sabri, K. Danapalasingam, and M. Rahmat, "A review on hybrid electric vehicles  
320        architecture and energy management strategies," *Renewable and Sustainable Energy Reviews*,  
321        vol. 53, pp. 1433-1442, 2016.
- 322    [7]    S. Onori, L. Serrao, and G. Rizzoni, *Hybrid electric vehicles: energy management strategies*:  
323        Springer, 2016.
- 324    [8]    Z. Lu, J. Song, S. Fang, F. Li, and L. Yu, "Shifting Control of Uninterrupted Multi-Speed  
325        Transmission Used in Electric Vehicle," in *ASME 2018 International Design Engineering  
326        Technical Conferences and Computers and Information in Engineering Conference*, 2018,  
327        pp. V003T01A039-V003T01A039.
- 328    [9]    J. Liang, Y. Zhang, J.-H. Zhong, and H. Yang, "A novel multi-segment feature fusion based  
329        fault classification approach for rotating machinery," *Mechanical Systems and Signal  
330        Processing*, vol. 122, pp. 19-41, 2019.
- 331    [10]    H. He, Z. Liu, L. Zhu, and X. Liu, "Dynamic coordinated shifting control of automated  
332        mechanical transmissions without a clutch in a plug-in hybrid electric vehicle," *Energies*, vol.  
333        5, pp. 3094-3109, 2012.
- 334    [11]    J. Liang, H. Yang, J. Wu, N. Zhang, and P. D. Walker, "Power-on shifting in dual input  
335        clutchless power-shifting transmission for electric vehicles," *Mechanism and Machine  
336        Theory*, vol. 121, pp. 487-501, 2018.
- 337    [12]    B. Gao, Q. Liang, Y. Xiang, L. Guo, and H. Chen, "Gear ratio optimization and shift control  
338        of 2-speed I-AMT in electric vehicle," *Mechanical Systems and Signal Processing*, vol. 50,  
339        pp. 615-631, 2015.
- 340    [13]    W. Yang, J. Liang, J. Yang, and N. Zhang, "Optimal control of a novel uninterrupted multi-  
341        speed transmission for hybrid electricmining trucks," *Proceedings of the Institution of  
342        Mechanical Engineers, Part D: Journal of Automobile Engineering*, p. 0954407018821524,  
343        2019.
- 344    [14]    Z. Yan, F. Yan, J. Liang, and Y. Duan, "Detailed modeling and experimental assessments of  
345        automotive dry clutch engagement," *IEEE Access*, pp. 1-1, 2019.
- 346    [15]    C.-Y. Tseng and C.-H. Yu, "Advanced shifting control of synchronizer mechanisms for  
347        clutchless automatic manual transmission in an electric vehicle," *Mechanism and Machine  
348        Theory*, vol. 84, pp. 37-56, 2015.

349 [16] J. Liang, H. Yang, J. Wu, N. Zhang, and P. D. Walker, "Shifting and power sharing control  
350 of a novel dual input clutchless transmission for electric vehicles," *Mechanical Systems and*  
351 *Signal Processing*, vol. 104, pp. 725-743, 2018.

352 [17] T. Holdstock, A. Sorniotti, M. Everitt, M. Fracchia, S. Bologna, and S. Bertolotto, "Energy  
353 consumption analysis of a novel four-speed dual motor drivetrain for electric vehicles," in  
354 *2012 IEEE Vehicle Power and Propulsion Conference*, 2012, pp. 295-300.

355 [18] S. Zhang, R. Xiong, C. Zhang, and F. Sun, "An optimal structure selection and parameter  
356 design approach for a dual-motor-driven system used in an electric bus," *Energy*, vol. 96, pp.  
357 437-448, 2016.

358 [19] J. Liang, P. D. Walker, J. Ruan, H. Yang, J. Wu, and N. Zhang, "Gearshift and brake  
359 distribution control for regenerative braking in electric vehicles with dual clutch  
360 transmission," *Mechanism and Machine Theory*, vol. 133, pp. 1-22, 2019.

361 [20] H. Wu, P. Walker, J. Wu, J. Liang, J. Ruan, and N. Zhang, "Energy management and shifting  
362 stability control for a novel dual input clutchless transmission system," *Mechanism and*  
363 *Machine Theory*, vol. 135, pp. 298-321, 2019.

364 [21] S. G. Wirasingha and A. Emadi, "Classification and review of control strategies for plug-in  
365 hybrid electric vehicles," *IEEE Transactions on vehicular technology*, vol. 60, pp. 111-122,  
366 2011.

367 [22] J. Peng, H. He, and R. Xiong, "Rule based energy management strategy for a series-parallel  
368 plug-in hybrid electric bus optimized by dynamic programming," *Applied Energy*, vol. 185,  
369 pp. 1633-1643, 2017.

370 [23] L. Serrao, S. Onori, and G. Rizzoni, "A comparative analysis of energy management  
371 strategies for hybrid electric vehicles," *Journal of Dynamic Systems, Measurement, and*  
372 *Control*, vol. 133, p. 031012, 2011.

373 [24] H. Yin, W. Zhou, M. Li, C. Ma, and C. Zhao, "An adaptive fuzzy logic-based energy  
374 management strategy on battery/ultracapacitor hybrid electric vehicles," *IEEE Transactions*  
375 *on Transportation Electrification*, vol. 2, pp. 300-311, 2016.

376 [25] C. Romaus, K. Gathmann, and J. Böcker, "Optimal energy management for a hybrid energy  
377 storage system for electric vehicles based on stochastic dynamic programming," in *Vehicle*  
378 *Power and Propulsion Conference (VPPC), 2010 IEEE*, 2010, pp. 1-6.

379 [26] S. Zhang and R. Xiong, "Adaptive energy management of a plug-in hybrid electric vehicle  
380 based on driving pattern recognition and dynamic programming," *Applied Energy*, vol. 155,  
381 pp. 68-78, 2015.

382 [27] G. Valenzuela, T. Kawabe, and M. Mukai, "Nonlinear model predictive control of battery  
383 electric vehicle with slope information," in *2014 IEEE International Electric Vehicle*  
384 *Conference (IEVC)*, 2014, pp. 1-5.

385 [28] L. Serrao, S. Onori, and G. Rizzoni, "ECMS as a realization of Pontryagin's minimum  
386 principle for HEV control," in *2009 American control conference*, 2009, pp. 3964-3969.

387 [29] T. Miro-Padovani, G. Colin, A. Ketfi-Chérif, and Y. Chamailard, "Implementation of an  
388 energy management strategy for hybrid electric vehicles including drivability constraints,"  
389 *IEEE Transactions on Vehicular Technology*, vol. 65, pp. 5918-5929, 2016.

390 [30] W. Yu, B. Li, H. Jia, M. Zhang, and D. Wang, "Application of multi-objective genetic  
391 algorithm to optimize energy efficiency and thermal comfort in building design," *Energy and*  
392 *Buildings*, vol. 88, pp. 135-143, 2015.  
393